Cramér-Rao Bound of Direction Finding Using Uniform Arc Arrays

Veronicah NYOKABI, Dominic Makaa KITAVI, and Cyrus Gitonga NGARI
Dept. of Mathematics, Computing and Information Technology,
University of Embu, Embu, Kenya.

***Abstract*— Direction-of-Arrival estimation accuracy using arc array geometry is considered in this paper. There is a scanty use of Uniform Arc Array (UAA) in conjunction with Cramér-Rao bound (CRB) for Direction-of-Arrival estimation. This paper proposed to use Uniform Arc Array formed from a considered Uniform Circular Array (UCA) in conjunction with CRB for Direction-of-Arrival estimation. This Uniform Arc Array is obtained by squeezing all sensors on the Uniform Circular Array circumference uniformly onto the Arc Array. Cramér-Rao bounds for the Uniform Arc Array and that of the Uniform Circular Array are derived. Comparison of performance of the Uniform Circular Array and Uniform Arc Array is done. It was observed that Uniform Arc Array has better estimation accuracy as compared to Uniform Circular Array when number of sensors equals four and five and azimuth angle ranging between $\frac{\pi}{9}$ and $\frac{7}{18}\pi$ and also $\frac{10}{9}\pi$ and $\frac{25}{18}\pi$. However, UCA and UAA have equal performance when the number of sensors equals three and the azimuth angle ranging between 0 and 2π. UCA has better estimation accuracy as compared to UAA when the number of sensors equals four and five and the azimuth angle ranging between $\frac{\pi}{2}$ and π and also $\frac{3}{2}\pi$ and 2π.**

***Index Terms*— array signal processing, direction-of-arrival estimation, direction finding, Cramér-Rao bound, uniform arc array.**

I Introduction

The general performance of any Direction Finding (DF) system is a function of both the DF algorithm used and array geometry [1]. Direction-of-Arrival (DOA)/Direction Finding (DF) is the direction in which an incoming signal arrives into an array of sensors (a group of sensors arranged/organized in a particular pattern). Direction-of-arrival (DOA) estimation is a fundamental problem in array signal processing. Various algorithms have been proposed for DOA estimation such as Multiple Signal Classification (MUSIC), Root-MUSIC, propagator methods, high-order cumulant method, Maximum Likelihood Method (MLM), among many others [2]. Its accuracy is an important parameter of any direction finding system [3]. Cramér-Rao bound is a very important tool for evaluating the accuracy of any parameter estimation method since it provides a lower bound on the accuracy of any unbiased estimator [3].

Performance of various estimators (MUSIC, MLE, among others) is compared to the ultimate performance corresponding to CRB [4]. Regardless of the specific algorithm used, CRB lower bounds estimation error variance of any unbiased estimator [5]. Therefore, CRB provides an algorithm-independent basis against which various algorithms are compared [3]. It has been used in several works such as Cramér-Rao bound for DF using an L-Shaped Array with Non-orthogonal Axes [6], accuracy limits through Cramér-Rao Lower Bound for Geolocation of Internet hosts [7], among many others.

One of the simplest array geometry which enables signal array-processing algorithms to be applied easily is the uniform linear array (ULA) [12]. It has useful properties such as application of forward-backward spatial smoothing to only ULA because of the Vandermonde structure of the array steering matrix, application of fast subspace algorithms such as Root-MUSIC in ULA, hence computational efficiency increment [13]. However, ULA will limit azimuth field of view below π (normally $\frac{2}{3}\pi$) since it is one-dimensional. The solution to this problem requires the use of several ULAs arranged in triangular or rectangular shape among others or rotating the ULA a few times to cover the entire azimuth spread. This use of several ULAs increases the cost as well as collecting a lot of data [14].

There are other geometries that have been employed to resolve the problem of the non-uniform performance of ULA in all directions which degrades Direction-of-Arrival (DOA) estimation performance in angles close to endfire [15]. In 2-dimension angle estimation, Uniform Circular Array (UCA) which is a geometrical pattern with a number of sensors equally spaced on the circumference of a circle is highly used due to its attractive advantages such as it provides a 2π full azimuth coverage, has an extra information on elevation angle and its direction pattern is almost unchanged [16]. However, UCA is expected to suffer serious mutual coupling effects because of the compelling coupling that can occur between elements that are positioned diametrically opposite one another together with the strong coupling between adjacent elements. This effect can be compensated since the symmetry of the UCA can break down into a series of symmetrical spatial components using the array excitation [12].

There are different array configurations/geometries in the literature used for DF such as linear, planar and conformal arrays [8]. Unfortunately, very little is known about the arrangement of sensors along a curve or an arc [10]. An arc is a portion or a part of the circumference of a circle. A uniform arc array is a geometrical pattern with a number of sensors equally spaced on an arc. Circular arcs were treated as very important features in the field of pattern recognition such as they were used for recognizing curved objects. They were also used as shape features for recognition purpose and closed circular arcs were used as local features in identifying and locating partially

occluded objects [11]. There is a scanty use of uniform arc array geometry for DOA estimation and therefore this paper proposed to form a uniform arc array (UAA) out of a uniform circular array to be considered for DOA estimation. This paper proposed to use a UCA with a known finite isotropic/identical number of sensors with a narrow-band far-field signal emitted by a single source arriving on the UCA. It is organized as follows; In Section II the array geometries (UCA and UAA) will be developed. In section III a statistical data model for the geometries will be assumed. In section IV the CRB of the suggested geometries will be derived. Section V will be analysis and section VII will be the conclusion.

II Development of the Array Geometries

II-A. Uniform Circular Array

A uniform circular array (UCA) with L number of isotropic sensors equally spaced on the circumference of the circle of radius R, at points S_1 to S_L is considered. These sensors will be considered to be arranged anticlockwise from the positive x-axis where the direction of arrangement does not matter since the sensors are identical. The Cartesian coordinate system origin is assumed to be the central point of the UCA array denoted as O. This point is considered as the reference point. A plane-wave signal from a far-field source is assumed to arrive on O at an azimuth angle ϕ measured anticlockwise from the positive x-axis, and a polar angle θ measured clockwise from the positive z-axis. See Figure 1.

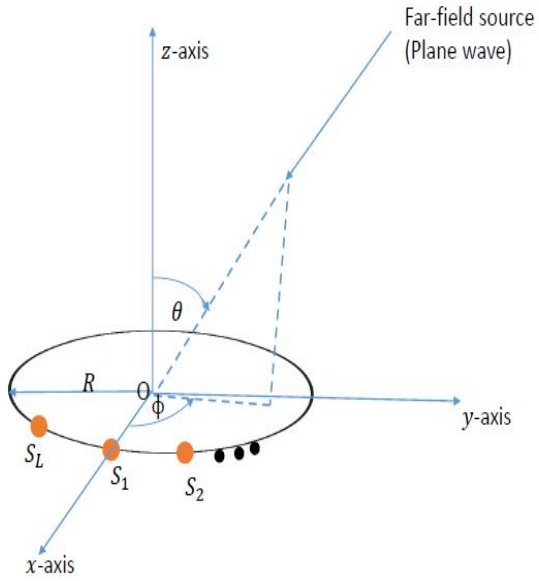

Fig. 1. Uniform Circular Array (UCA).

The position vector for the ℓ^{th} sensor on the UCA, $\mathbf{p}_\ell$, is given by [9]

$$\mathbf{p}_\ell = \left[R\cos\left(\tfrac{2\pi(\ell-1)}{L}\right), R\sin\left(\tfrac{2\pi(\ell-1)}{L}\right), 0\right]^T \quad (1)$$

and the array manifold vector for the UCA is

$$\mathbf{a}_{\text{UCA}} = \begin{bmatrix} \exp\left\{i\frac{2\pi R}{\lambda}\sin(\theta)\cos(\phi)\right\} \\ \exp\left\{i\frac{2\pi R}{\lambda}\sin(\theta)\cos(\phi-\frac{2\pi}{L})\right\} \\ \exp\left\{i\frac{2\pi R}{\lambda}\sin(\theta)\cos(\phi-\frac{4\pi}{L})\right\} \\ \vdots \\ \exp\left\{i\frac{2\pi R}{\lambda}\sin(\theta)\cos\left(\phi-\frac{2\pi(L-1)}{L}\right)\right\} \end{bmatrix}. \quad (2)$$

II-B. Uniform Arc Array

A uniform arc array (UAA) from the UCA formed by squeezing all L number of sensors onto an arc of a known angle is considered. The sensors are arranged anticlockwise from the positive x-axis. See Figure 2.

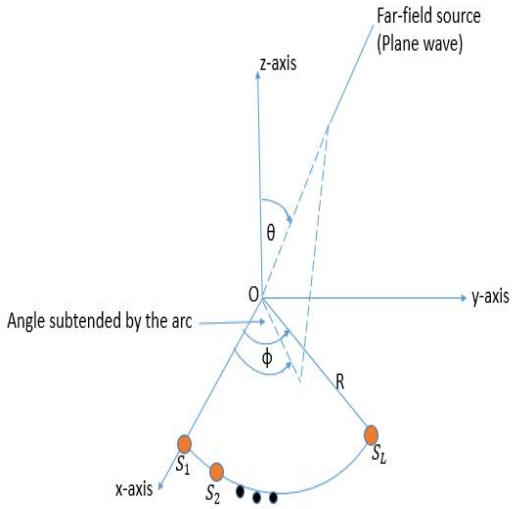

Fig. 2. Uniform Arc Array (UAA).

The position vector for the ℓ^{th} sensor on the UAA, $\mathbf{p}_\ell$, is given by

$$\mathbf{p}_\ell = \left[R\cos\left(\tfrac{2\pi(\ell-1)}{L(L-1)}\right), R\sin\left(\tfrac{2\pi(\ell-1)}{L(L-1)}\right), 0\right]^T \quad (3)$$

and the corresponding array manifold vector is given by

$$\mathbf{a}_{\text{UAA}} = \begin{bmatrix} \exp\left\{i\frac{2\pi R}{\lambda}\sin(\theta)\cos(\phi)\right\} \\ \exp\left\{i\frac{2\pi R}{\lambda}\sin(\theta)\cos\left(\phi-\frac{2\pi}{L(L-1)}\right)\right\} \\ \exp\left\{i\frac{2\pi R}{\lambda}\sin(\theta)\cos\left(\phi-\frac{4\pi}{L(L-1)}\right)\right\} \\ \vdots \\ \exp\left\{i\frac{2\pi R}{\lambda}\sin(\theta)\cos\left(\phi-\frac{2\pi}{L}\right)\right\} \end{bmatrix}. \quad (4)$$

III Statistical Data Model

Signals impinging on the array of sensors from a certain source are affected/corrupted by additive noise. Thus, at the array of sensors, the observed data for the geometry used is given by [6]

$$\mathbf{z}(m) = \mathbf{a}(\theta,\phi)s(m) + \mathbf{n}(m),\ m = 1,2,...,M; \quad (5)$$

where $s(m)$ is the signal received at m^{th} time instant and $\boldsymbol{n}(m)$ is the additive noise. From the model, $\boldsymbol{n}(m)$, $\boldsymbol{z}(m)$

and $\mathbf{a}(\theta,\phi)$ will be $L\times 1$ vectors. For multiple time instants/snapshots M, the data model vector will be given by [6]

$$\tilde{\mathbf{z}} = \mathbf{s}\otimes\mathbf{a}(\theta,\phi)+\tilde{\mathbf{n}} \quad (6)$$

where

$$\begin{aligned}\tilde{\mathbf{z}} &= [\mathbf{z}(1),\mathbf{z}(2),\cdots,\mathbf{z}(M)]^T,\\ \mathbf{s} &= [s(1),s(2),\cdots,s(M)]^T,\\ \tilde{\mathbf{n}} &= [\mathbf{n}(1),\mathbf{n}(2),\cdots,\mathbf{n}(M)]^T,\end{aligned}$$

and $\otimes$ is the Kronecker product.

For simplicity, a pure-tone incident signal $s(m) = \sigma_{_s}\exp[j(2\pi fm+\varphi)]$ will be considered, where $\sigma_{_s}$ is the signals' amplitude and φ is the phase angle.

The random variables $\mathbf{z}(1),\mathbf{z}(2),\cdots,\mathbf{z}(M)$ are assumed to be independent and have the same probability distribution. Therefore, the random variable $\tilde{\mathbf{z}}$ has a mean of $\boldsymbol{\mu}(\theta,\phi)$ and a covariance matrix of $\boldsymbol{\Gamma}(\theta,\phi)$ hence it follows a normal distribution $\mathbf{z}\sim\mathcal{N}(\boldsymbol{\mu},\boldsymbol{\Gamma})$ which has a probability density function (likelihood function) $p(\tilde{\mathbf{z}}|\Theta)$ where $\Theta=\{\theta,\phi\}$, i.e.

$$p(\tilde{\mathbf{z}}|\Theta) = \frac{1}{\sqrt{|2\pi\boldsymbol{\Gamma}|}}\exp\left\{-\frac{1}{2}[\tilde{\mathbf{z}}-\boldsymbol{\mu}]^H\boldsymbol{\Gamma}^{-1}[\tilde{\mathbf{z}}-\boldsymbol{\mu}]\right\}. \quad (7)$$

In the above, $\boldsymbol{\mu}=E[\tilde{\mathbf{z}}]$, $\boldsymbol{\Gamma}=E\left\{[\tilde{\mathbf{z}}-\boldsymbol{\mu}][\tilde{\mathbf{z}}-\boldsymbol{\mu}]^H\right\}$ and $|\cdot|$ denotes the corresponding matrix determinant.

$$\begin{aligned}\boldsymbol{\mu} &= E[\tilde{\mathbf{z}}] = E[\boldsymbol{s}\otimes\mathbf{a}(\theta,\phi)+\tilde{n}]\\ &= E[\mathbf{s}\otimes\mathbf{a}(\theta,\phi)]+E[\tilde{\mathbf{n}}]\\ &= \mathbf{s}\otimes\mathbf{a}(\theta,\phi) \quad (8)\end{aligned}$$

and

$$\begin{aligned}\boldsymbol{\Gamma} &= E\left\{[\tilde{\mathbf{z}}-\boldsymbol{\mu}][\tilde{\mathbf{z}}-\boldsymbol{\mu}]^H\right\}\\ &= E[\tilde{\mathbf{n}}\tilde{\mathbf{n}}^H]\\ &= \sigma_{_n}^2\mathbf{I}_{ML\times ML}. \quad (9)\end{aligned}$$

IV Derivation of the Cramér-Rao Bound

To get the Cramér-Rao bound, the inverse of the Fisher Information Matrix (FIM) is obtained. Since the observed data vector, in this case, is complex-valued, a simplified FIM for multivariate normal distribution is given by [6]

$$\begin{aligned}[\mathbf{F}(\boldsymbol{\xi})]_{k,r} &= 2\mathrm{Re}\left\{\left[\frac{\partial\boldsymbol{\mu}}{\partial\boldsymbol{\xi}_k}\right]^H\boldsymbol{\Gamma}^{-1}\frac{\partial\boldsymbol{\mu}}{\partial\boldsymbol{\xi}_r}\right\}\\ &\quad +\mathrm{Tr}\left\{\boldsymbol{\Gamma}^{-1}\frac{\partial\boldsymbol{\Gamma}}{\partial\boldsymbol{\xi}_k}\boldsymbol{\Gamma}^{-1}\frac{\partial\boldsymbol{\Gamma}}{\partial\boldsymbol{\xi}_r}\right\}. \quad (10)\end{aligned}$$

In the above, $\mathrm{Re}\{\cdot\}$ indicates the real part of the identity inside the curly brackets, $\boldsymbol{\xi}=[\theta,\phi]$ is the set of unknown parameters and $k,r=\{1,2\}$.

IV-A. Cramér-Rao Bound for the Uniform Circular Array

The FIM here will be given by [6]

$$\mathbf{F}(\boldsymbol{\xi}) = \begin{bmatrix}[\mathbf{F}(\boldsymbol{\xi})]_{1,1} & [\mathbf{F}(\boldsymbol{\xi})]_{1,2}\\ [\mathbf{F}(\boldsymbol{\xi})]_{2,1} & [\mathbf{F}(\boldsymbol{\xi})]_{2,2}\end{bmatrix} \quad (11)$$

and therefore computing the entries of the FIM one by one we have,

Using (2), (8) and (9) in (10), we have

$$[\mathbf{F}(\boldsymbol{\xi})]_{1,1} = ML\left(\frac{2\pi R\sigma_{_s}}{\lambda\sigma_{_n}}\right)^2\cos^2(\theta), \quad (12)$$

$$[\mathbf{F}(\boldsymbol{\xi})]_{2,2} = ML\left(\frac{2\pi R\sigma_{_s}}{\lambda\sigma_{_n}}\right)^2\sin^2(\theta), \quad (13)$$

$$\begin{aligned}[\mathbf{F}(\boldsymbol{\xi})]_{1,2} &= [\mathbf{F}(\boldsymbol{\xi})]_{2,1}\\ &= 0. \quad (14)\end{aligned}$$

Thus,

$$\mathbf{F}(\boldsymbol{\xi}) = ML\left(\frac{2\pi R\sigma_{_s}}{\lambda\sigma_{_n}}\right)^2\begin{bmatrix}\cos^2(\theta) & 0\\ 0 & \sin^2(\theta)\end{bmatrix}. \quad (15)$$

Hence, Cramér-Rao bounds for the UCA are

$$\mathrm{CRB}_{\mathrm{UCA}}(\theta) = \frac{1}{ML}\left(\frac{\lambda\sigma_{_n}}{2\pi R\sigma_{_s}}\right)^2\sec^2\theta \quad (16)$$

and

$$\mathrm{CRB}_{\mathrm{UCA}}(\phi) = \frac{1}{ML}\left(\frac{\lambda\sigma_{_n}}{2\pi R\sigma_{_s}}\right)^2\csc^2\theta. \quad (17)$$

IV-B. Cramér-Rao Bound for the Uniform Arc Array

Using (4), (8) and (9) in (10), we have

$$[\mathbf{F}(\boldsymbol{\xi})]_{1,1} = 8M\left\{\frac{\pi R\sigma_{_s}}{\lambda\sigma_{_n}}\right\}^2\left\{\frac{L}{2}+D\right\}\cos^2(\theta), \quad (18)$$

$$\begin{aligned}[\mathbf{F}(\boldsymbol{\xi})]_{1,2} &= [\mathbf{F}(\boldsymbol{\xi})]_{2,1}\\ &= -8M\left\{\frac{\pi R\sigma_s}{\lambda\sigma_{_n}}\right\}^2\{F\}\sin(\theta)\cos(\theta), \quad (19)\end{aligned}$$

$$[\mathbf{F}(\boldsymbol{\xi})]_{2,2} = 8M\left\{\frac{\pi R\sigma_{_s}}{\lambda\sigma_{_n}}\right\}^2\left\{\frac{L}{2}-E\right\}\sin^2(\theta), \quad (20)$$

where

$$D = \frac{\sin\left(\frac{2\pi}{L-1}\right)\cos\left(\frac{2\pi}{L}-2\phi\right)}{2\sin\left(\frac{2\pi}{L(L-1)}\right)},$$

$$E = \frac{\sin\left(\frac{2\pi}{L-1}\right)\cos\left(\frac{2\pi}{L}+2\phi\right)}{2\sin\left(\frac{2\pi}{L(L-1)}\right)},$$

$$F = \frac{-\sin\left(\frac{2\pi}{L-1}\right)\sin\left(-\frac{2\pi}{L}+2\phi\right)}{2\sin\left(\frac{2\pi}{L(L-1)}\right)}.$$

The Cramér-Rao bounds become

$$\mathrm{CRB}_{\mathrm{UAA}}(\theta) = \frac{\lambda^2\sigma_{_n}^2\sec^2(\theta)\gamma}{8\pi^2MR^2\sigma_{_s}^2\beta} \quad (21)$$

and

$$\mathrm{CRB}_{\mathrm{UAA}}(\phi) = \frac{\lambda^2\sigma_n^2\csc^2(\theta)\alpha}{8\pi^2MR^2\sigma_s^2\beta} \quad (22)$$

where

$$\begin{aligned}\gamma &= \frac{L}{2}-E,\\ &= \frac{L-\sin\left(\frac{2\pi}{L-1}\right)\csc\left(\frac{2\pi}{L(L-1)}\right)\cos\left(\frac{2\pi}{L}+2\phi\right)}{2}, \quad (23)\end{aligned}$$

$$\begin{aligned}\alpha &= \frac{L}{2}+D,\\ &= \frac{L+\sin\left(\frac{2\pi}{L-1}\right)\csc\left(\frac{2\pi}{L(L-1)}\right)\cos\left(\frac{2\pi}{L}-2\phi\right)}{2}, \quad (24)\end{aligned}$$

$$\begin{aligned}\beta &= \left(\frac{L}{2}+D\right)\left(\frac{L}{2}-E\right)-F^2\\ &= \frac{1}{4}\left\{L-\sin\left(\frac{2\pi}{L-1}\right)\csc\left(\frac{2\pi}{L(L-1)}\right)\right\}\\ &\quad\times\frac{1}{4}\left\{\cos\left(\frac{2\pi}{L}+2\phi\right)\right\}\\ &\quad\times\left\{L+\sin\left(\frac{2\pi}{L-1}\right)\csc\left(\frac{2\pi}{L(L-1)}\right)\right\}\\ &\quad\times\left\{\cos\left(\frac{2\pi}{L}-2\phi\right)\right\}\\ &\quad-\frac{1}{4}\left\{\sin\left(\frac{2\pi}{L-1}\right)\csc\left(\frac{2\pi}{L(L-1)}\right)\right\}^2\\ &\quad\times\frac{1}{4}\left\{\sin\left(-\frac{2\pi}{L}+2\phi\right)\right\}^2. \quad (25)\end{aligned}$$

V Analysis

V-A. CRB for the Elevation Angle θ

From equations (16), (21), (23) and (25)

$$\begin{aligned}&\frac{\mathrm{CRB}_{\mathrm{UCA}}(\theta)}{\mathrm{CRB}_{\mathrm{UAA}}(\theta)}\\ =\ &\frac{2\beta}{L\gamma}\\ =\ &\left\{\frac{L+\sin\left(\frac{2\pi}{L-1}\right)\csc\left(\frac{2\pi}{L(L-1)}\right)\cos\left(\frac{2\pi}{L}-2\phi\right)}{L}\right\}\\ &-\frac{\left\{\sin\left(\frac{2\pi}{L-1}\right)\csc\left(\frac{2\pi}{L(L-1)}\right)\sin\left(-\frac{2\pi}{L}+2\phi\right)\right\}^2}{L\left\{L-\sin\left(\frac{2\pi}{L-1}\right)\csc\left(\frac{2\pi}{L(L-1)}\right)\cos\left(\frac{2\pi}{L}+2\phi\right)\right\}}\\ =\ &\frac{L+T_1}{L}-\frac{{T_2}^2}{LT_3} \quad (26)\end{aligned}$$

where,

$$\begin{aligned}T_1 &= \sin\left(\frac{2\pi}{L-1}\right)\csc\left(\frac{2\pi}{L(L-1)}\right)\cos\left(\frac{2\pi}{L}-2\phi\right),\\ T_2 &= \sin\left(\frac{2\pi}{L-1}\right)\csc\left(\frac{2\pi}{L(L-1)}\right)\sin\left(-\frac{2\pi}{L}+2\phi\right),\\ T_3 &= L-\sin\left(\frac{2\pi}{L-1}\right)\csc\left(\frac{2\pi}{L(L-1)}\right)\cos\left(\frac{2\pi}{L}+2\phi\right).\end{aligned}$$

V-A.1. When $\frac{\mathrm{CRB}_{\mathrm{UCA}}(\theta)}{\mathrm{CRB}_{\mathrm{UAA}}(\theta)}<1$*:* From (26) we have

$$\frac{L+T_1}{L}-\frac{{T_2}^2}{LT_3}<1 \quad (27)$$

which implies

$$T_1T_3<{T_2}^2. \quad (28)$$

This means that UCA has better estimation accuracy as compared to UAA for $L=4,5$, $\frac{\pi}{2}\le\phi\le\pi$ and $\frac{3}{2}\pi\le\phi\le2\pi$.

V-A.2. When $\frac{\mathrm{CRB}_{\mathrm{UCA}}(\theta)}{\mathrm{CRB}_{\mathrm{UAA}}(\theta)}=1$*:* From (26) we have

$$\frac{L+T_1}{L}-\frac{{T_2}^2}{LT_3}=1 \quad (29)$$

which implies

$$T_1T_3={T_2}^2. \quad (30)$$

This means that UAA and UCA have same performance for $L=3$ and $0\le\phi\le2\pi$.

V-A.3. When $\frac{\mathrm{CRB}_{\mathrm{UCA}}(\theta)}{\mathrm{CRB}_{\mathrm{UAA}}(\theta)}>1$*:* From (26) we have

$$\frac{L+T_1}{L}-\frac{{T_2}^2}{LT_3}>1 \quad (31)$$

which implies

$$T_1T_3>{T_2}^2. \quad (32)$$

This means that UAA has better estimation accuracy as compared to UCA for $L=4,5$, $\frac{\pi}{9}\le\phi\le\frac{7}{18}\pi$ and $\frac{10}{9}\pi\le\phi\le\frac{25}{18}\pi$.

V-B. CRB for the Azimuth Angle ϕ

From equations (17), (22), (24) and (25)

$$\begin{aligned}
&\frac{\mathrm{CRB}_{\mathrm{UCA}}(\phi)}{\mathrm{CRB}_{\mathrm{UAA}}(\phi)} \\
&= \frac{2\beta}{L\alpha} \\
&= \left\{\frac{L-\sin\left(\frac{2\pi}{L-1}\right)\csc\left(\frac{2\pi}{L(L-1)}\right)\cos\left(\frac{2\pi}{L}+2\phi\right)}{L}\right\} \\
&\quad -\frac{\left\{\sin\left(\frac{2\pi}{L-1}\right)\csc\left(\frac{2\pi}{L(L-1)}\right)\sin\left(-\frac{2\pi}{L}+2\phi\right)\right\}^2}{L\left\{L+\sin\left(\frac{2\pi}{L-1}\right)\csc\left(\frac{2\pi}{L(L-1)}\right)\cos\left(\frac{2\pi}{L}-2\phi\right)\right\}} \\
&= \frac{L-T_4}{L}-\frac{{T_2}^2}{LT_5} \qquad (33)
\end{aligned}$$

where,

$$\begin{aligned}
T_4 &= \sin\left(\frac{2\pi}{L-1}\right)\csc\left(\frac{2\pi}{L(L-1)}\right)\cos\left(\frac{2\pi}{L}+2\phi\right), \\
T_2 &= \sin\left(\frac{2\pi}{L-1}\right)\csc\left(\frac{2\pi}{L(L-1)}\right)\sin\left(-\frac{2\pi}{L}+2\phi\right), \\
T_5 &= L+\sin\left(\frac{2\pi}{L-1}\right)\csc\left(\frac{2\pi}{L(L-1)}\right)\cos\left(\frac{2\pi}{L}-2\phi\right).
\end{aligned}$$

V-B.1. When $\frac{\mathrm{CRB}_{\mathrm{UCA}}(\phi)}{\mathrm{CRB}_{\mathrm{UAA}}(\phi)} < 1$*:* From (33) we have

$$\frac{L-T_4}{L}-\frac{{T_2}^2}{LT_5} < 1 \qquad (34)$$

which implies

$$-T_4T_5 < {T_2}^2. \qquad (35)$$

This means that UCA has better estimation accuracy as compared to UAA for $L = 4, 5$, $\frac{\pi}{2} \le \phi \le \pi$ and $\frac{3}{2}\pi \le \phi \le 2\pi$.

V-B.2. When $\frac{\mathrm{CRB}_{\mathrm{UCA}}(\phi)}{\mathrm{CRB}_{\mathrm{UAA}}(\phi)} = 1$*:* From (33) we have

$$\frac{L-T_4}{L}-\frac{{T_2}^2}{LT_5} = 1 \qquad (36)$$

which implies

$$-T_4T_5 = {T_2}^2. \qquad (37)$$

This means that UAA and UCA have same performance for $L = 3$ and $0 \le \phi \le 2\pi$.

V-B.3. When $\frac{\mathrm{CRB}_{\mathrm{UCA}}(\phi)}{\mathrm{CRB}_{\mathrm{UAA}}(\phi)} > 1$*:* From (33) we have

$$\frac{L-T_4}{L}-\frac{{T_2}^2}{LT_5} > 1 \qquad (38)$$

which implies

$$-T_4T_5 > {T_2}^2. \qquad (39)$$

This means that UAA has better estimation accuracy as compared to UCA for $L = 4, 5$, $\frac{\pi}{9} \le \phi \le \frac{7}{18}\pi$ and $\frac{10}{9}\pi \le \phi \le \frac{25}{18}\pi$.

VI Numerical Simulations

The following diagrams validates the numerical results in section (V).

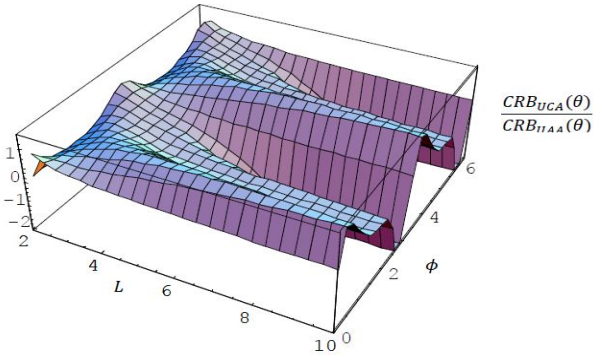

Fig. 3. Comparison of $\mathrm{CRB}_{\mathrm{UCA}}(\theta)$ and $\mathrm{CRB}_{\mathrm{UAA}}(\theta)$.

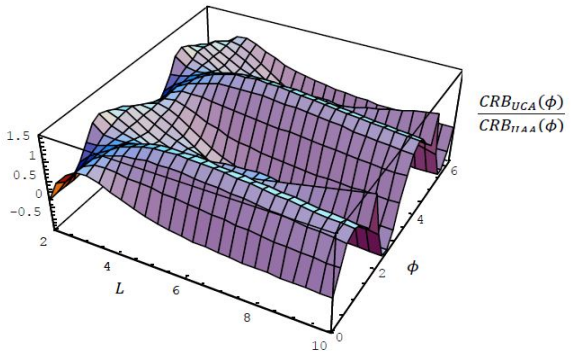

Fig. 4. Comparison of $\mathrm{CRB}_{\mathrm{UCA}}(\phi)$ and $\mathrm{CRB}_{\mathrm{UAA}}(\phi)$.

Ratios (26) and (33) are discontinuous when $\csc\left(\frac{2\pi}{L(L-1)}\right) = \infty$ at which points $\sin\left(\frac{2\pi}{L(L-1)}\right) = 0$.

VI-A. The Special Cases of $\frac{\mathrm{CRB}_{\mathrm{UCA}}(\theta)}{\mathrm{CRB}_{\mathrm{UAA}}(\theta)}$ and $\frac{\mathrm{CRB}_{\mathrm{UCA}}(\phi)}{\mathrm{CRB}_{\mathrm{UAA}}(\phi)}$

VI-A.1. $\frac{\mathrm{CRB}_{\mathrm{UCA}}(\theta)}{\mathrm{CRB}_{\mathrm{UAA}}(\theta)} < 1$ *and* $\frac{\mathrm{CRB}_{\mathrm{UCA}}(\phi)}{\mathrm{CRB}_{\mathrm{UAA}}(\phi)} < 1$*:* When $L = 4$ and 5 and $\frac{\pi}{2} \le \phi \le \pi$, then from equations (26) and (33) we obtain Figure 5.

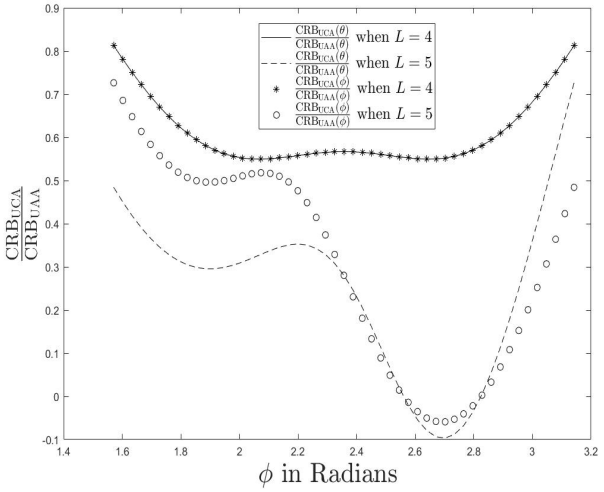

Fig. 5. $\frac{\mathrm{CRB_{UCA}}(\theta)}{\mathrm{CRB_{UAA}}(\theta)} < 1$ and $\frac{\mathrm{CRB_{UCA}}(\phi)}{\mathrm{CRB_{UAA}}(\phi)} < 1$ when $L = 4$ and 5 and $\frac{\pi}{2} \leq \phi \leq \pi$

When $L = 4$ and 5 and $\frac{3}{2}\pi \leq \phi \leq 2\pi$, then from equations (26) and (33) we obtain Figure 6.

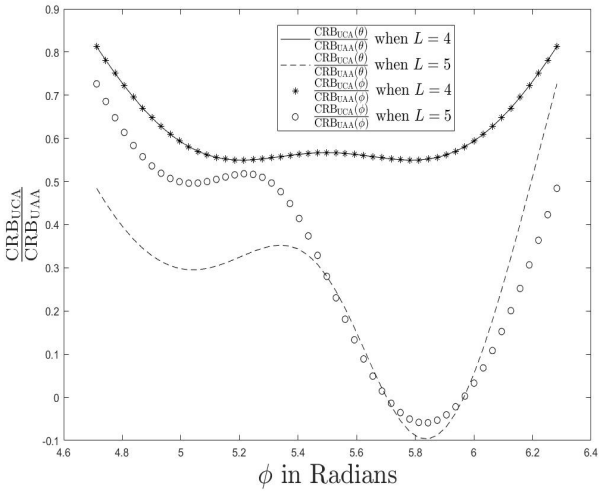

Fig. 6. $\frac{\mathrm{CRB_{UCA}}(\theta)}{\mathrm{CRB_{UAA}}(\theta)} < 1$ and $\frac{\mathrm{CRB_{UCA}}(\phi)}{\mathrm{CRB_{UAA}}(\phi)} < 1$ when $L = 4$ and 5 and $\frac{3}{2}\pi \leq \phi \leq 2\pi$

From Figures 5-6, it is clear that when $L = 4$ and 5, $\frac{\pi}{2} \leq \phi \leq \pi$ and $\frac{3}{2}\pi \leq \phi \leq 2\pi$, the ratios (26) and (33) are less than 1.

VI-A.2. $\frac{\mathrm{CRB_{UCA}}(\theta)}{\mathrm{CRB_{UAA}}(\theta)} > 1$ *and* $\frac{\mathrm{CRB_{UCA}}(\phi)}{\mathrm{CRB_{UAA}}(\phi)} > 1$*:* When $L = 4$ and 5 and $\frac{\pi}{9} \leq \phi \leq \frac{7}{18}\pi$, then from equations (26) and (33) we obtain Figure 7.

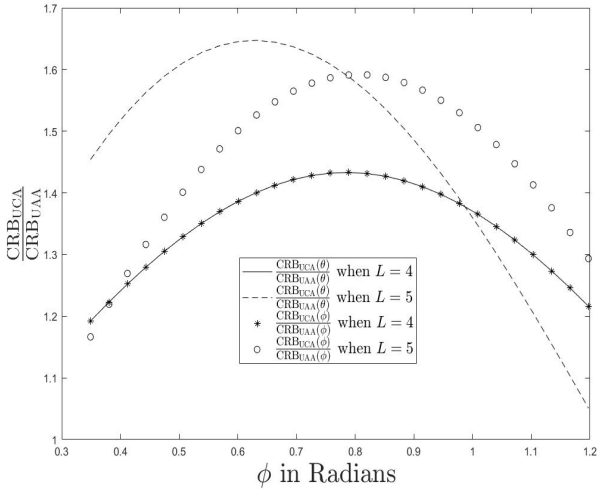

Fig. 7. $\frac{\mathrm{CRB_{UCA}}(\theta)}{\mathrm{CRB_{UAA}}(\theta)} > 1$ and $\frac{\mathrm{CRB_{UCA}}(\phi)}{\mathrm{CRB_{UAA}}(\phi)} > 1$ when $L = 4$ and 5 and $\frac{\pi}{9} \leq \phi \leq \frac{7}{18}\pi$

When $L = 4$ and 5 and $\frac{10}{9}\pi \leq \phi \leq \frac{25}{18}\pi$, then from equations (26) and (33) we obtain Figure 8.

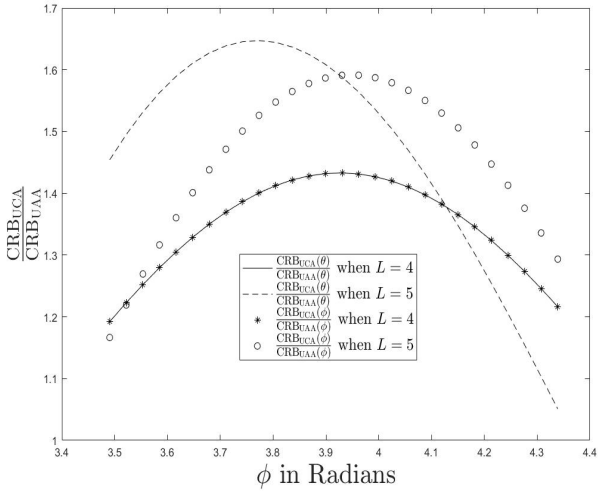

Fig. 8. $\frac{\mathrm{CRB_{UCA}}(\theta)}{\mathrm{CRB_{UAA}}(\theta)} > 1$ and $\frac{\mathrm{CRB_{UCA}}(\phi)}{\mathrm{CRB_{UAA}}(\phi)} > 1$ when $L = 4$ and 5 and $\frac{10}{9}\pi \leq \phi \leq \frac{25}{18}\pi$

From Figures 7-8, it is also clear that when $L = 4$ and 5, $\frac{\pi}{9} \leq \phi \leq \frac{7}{18}\pi$ and $\frac{10}{9}\pi \leq \phi \leq \frac{25}{18}\pi$, the ratios (26) and (33) are greater than 1.

VI-A.3. $\frac{\mathrm{CRB_{UCA}}(\theta)}{\mathrm{CRB_{UAA}}(\theta)} = 1$ *and* $\frac{\mathrm{CRB_{UCA}}(\phi)}{\mathrm{CRB_{UAA}}(\phi)} = 1$ *:* This case was only possible for $L = 3$ and $0 \leq \phi \leq 2\pi$ and therefore from equations (26) and (33) we obtain Figure 9.

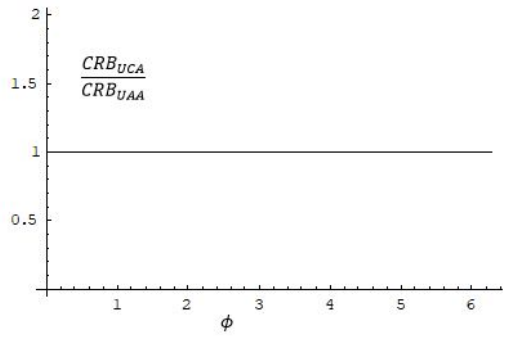

Fig. 9. $\frac{\mathrm{CRB}_{\mathrm{UCA}}(\theta)}{\mathrm{CRB}_{\mathrm{UAA}}(\theta)} = 1$ and $\frac{\mathrm{CRB}_{\mathrm{UCA}}(\phi)}{\mathrm{CRB}_{\mathrm{UAA}}(\phi)} = 1$ when $L = 3$ and $0 \leq \phi \leq 2\pi$

From Figure 9 it is clear that when $L = 3$ and $0 \leq \phi \leq 2\pi$ for both θ and ϕ, ratios (26) and (33) are equal to one.

VII Conclusion

The CRBs for both UCA and UAA were derived. Comparison of performance was done by getting the ratio of the obtained CRBs for both elevation angle and azimuth angle. The ratio of the CRB of UCA to the CRB of UAA for both elevation angle and azimuth angle being less than one implied that UCA has better estimation accuracy as compared to UAA.The ratio of the CRB of UCA to that of UAA for both elevation angle and azimuth angle being equals to one implied that UCA and UAA have equal performance. The ratio of the CRB of UCA to that of UAA for both elevation angle and azimuth angle being greater than one implied that UAA has better estimation accuracy as compared to UCA. Therefore, the proposed Uniform Arc Array has better estimation accuracy as compared to Uniform Circular Array when number of sensors equals four and five and azimuth angle ranging between $\frac{\pi}{9}$ and $\frac{7}{18}\pi$ and also $\frac{10}{9}\pi$ and $\frac{25}{18}\pi$. Future studies can focus on better estimation accuracy when the number of sensors increases.

References

[1] A. Manikas, A. Sleiman, and I. Dacos, "Manifold studies of nonlinear antenna array geometries," *IEEE Transactions on Signal Processing*, vol. 49, no. 3, pp. 497-505, 2001.

[2] Z. Xiaofei, L. Jianfeng, and X. Lingyun, "Novel two-dimensional DOA estimation with L-shaped array," *EURASIP Journal on Advances in Signal Processing*, no. 1, p. 50, 2011.

[3] T. E. Tuncer and B. Friedlander, editors. *Classical and Modern Direction-of-Arrival Estimation*. Academic Press, 2009.

[4] P. Stoica and A. Nehorai, "MUSIC, Maximum Likelihood, and Cramér-Rao bound: Further Results and Comparisons," *IEEE Transactions on Acoustics, Speech, and Signal Processing*, vol. 38, no. 12, pp. 2140-2150, 1990.

[5] P. K. Tam and K. T. Wong, "Cramér-Rao bounds for Direction Finding by an Acoustic Vector Sensor Under Nonideal Gain-Phase Responses, Noncollocation, or Nonorthogonal Orientation," *IEEE Sensors Journal*, vol. 9, no. 8, pp. 969-982, 2009.

[6] D. M. Kitavi, K. W. Thomas, and H. Chun-Chiu, "An L-Shaped Array With Nonorthogonal Axes-Its Cramér-Rao bound for Direction Finding 2 3 Ifa," *IEEE Transactions on Aerospace and Electronic Systems*, vol. 00, no. 10, pp. 1-8, 2017.

[7] G. Ciavarrini, M. S. Greco, and A. Vecchio, "Geolocation of Internet hosts: accuracy limits through Cramér-Rao Lower Bound," *Computer Networks*, 2018.

[8] W. H. Kummer, "Basic Array Theory," *Proceedings of the IEEE*, vol. 80, no. 1, pp. 127-140, 1992.

[9] H. L. Van. Trees, *optimum array processing part IV Detection, Estimation, and Modulation Theory*. John Wiley and Sons, 2004.

[10] S. Lee and Y. Lo, "On the Pattern Function of Circular Arc Arrays," *IEEE Transactions on Antennas and Propagaton*, vol. 13, no. 4, pp. 649-650, 1965.

[11] K. B. Lim, K. Xin, and G. S. Hong, "Detection and estimation of circular arc segments," *Pattern Recognition Letters*, vol. 16, no. 6, pp. 627-636, 1995.

[12] P. Ioannides and C. A. Balanis, "Uniform circular and rectangular arrays for adaptive beamforming applications," *IEEE Antennas and Wireless Propagation Letters*, vol. 4, no. 1, pp. 351-354, 2005.

[13] T. E. Tuncer, T. K. Yasar, and B. Friedlander, *Narrowband and Wideband DOA Estimation for Uniform and Nonuniform Linear Arrays*, 1^{st} ed. Elsevier, 2009.

[14] C. M. Tan, P. Fletcher, M. Beach, a R. Nix, M. Landmann, and R. S. Thom, "On the Application of Circular Arrays in Direction Finding Part I: Investigation into the estimation algorithms," *1st Annual COST 273 Workshop, Espoo, Finland, 29-30 May 2002*, no. May, pp. 29-30, 2002.

[15] S. Shirvani-Moghaddam and F. Akbari, "A novel ULA-based geometry for improving AOA estimation," *EURASIP Journal on Advances in Signal Processing*, no. 1, p. 39, 2011.

[16] Y. Wu and H. C. So, "Simple and accurate two-dimensional angle estimation for a single source with uniform circular array," *IEEE Antennas and Wireless Propagation Letters*, vol. 7, no. May 2014, pp. 78-80, 2008.

[17] B. R. Jackson, S. Rajan, Liao, J. Bruce, and S. Wang, "Direction of arrival estimation using directive antennas in uniform circular arrays," *IEEE Transactions on Antennas and Propagation*, vol. 63, no. 2, pp. 736-747, 2015.

[18] Z. Ye, L. Xiang, and X. Xu, "DOA estimation with circular array via spatial averaging algorithm," *IEEE Antennas and Wireless Propagation Letters*, vol. 6, no. 6, pp. 74-76, 2007.

[19] F. Belloni and V. Koivunen, "Unitary root-MUSIC technique for uniform circular array," *Proceedings of the 3rd IEEE International Symposium on Signal Processing and Information Technology, ISSPIT 2003*, pp. 451-454, 2003.

[20] L. Z. Xiang1, X. Ye1, C. Xu1, W. Chang2, Y. S. Xu2, and Hung2, "Direction of arrival estimation for uniform circular array based on fourth-order cumulants in the presence of unknown mutual coupling," *European Space Agency, (Special Publication) ESA SP*, vol. 626 SP, no. 3, pp. 281-287, 2008.

[21] C. Qi, Y. Wang, Y. Zhang, and H. Chen, "DOA estimation and self-calibration algorithm for uniform circular array," *Transactions of the Korean Institute of Electrical Engineers*, 2005.

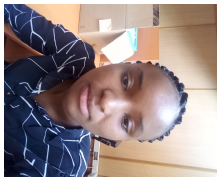

Veronicah NYOKABI obtained a B.Sc. (first-class honours) in B.S.c Science in 2016 from Embu University College a constituent of University of Nairobi (Kenya).

V. Nyokabi is currently pursuing M.Sc. in Applied Mathematics from the University of Embu (Kenya).

V. Nyokabi is a Graduate Assistant at University of Embu (Embu, Kenya) since January 2017.

V. Nyokabi's research interest lies in statistical signal processing and partial differential equations.

Dominic Makaa KITAVI obtained the B.Sc. (first-class honours) in Mathematics in 2011 from the University of Nairobi (Kenya), M.Sc. (cum laude) in Mathematical Sciences in 2013 from the University of Western Cape (South Africa), and Ph.D. in Electronic and Information Engineering, at the Hong Kong Polytechnic University (Hong Kong) in 2017.

D. M. Kitavi also obtained Certified Public Accountant one (CPA 1) from KASNEB (Kenya) in 2008.

D. M. Kitavi was an Accounts Assistant in Twiga Chemical Industries Limited (Nairobi, Kenya) in 2011-2012, and Assistant Lecturer at Mount Kenya University (Mombasa, Kenya) in 2014. Since September 2017, D. M. Kitavi has been with the University of Embu (Kenya) as a Lecturer.

D. M. Kitavi's research interest lies in statistical signal processing and partial differential equations.

Cyrus Gitonga NGARI obtained a second class honours (upper division) in B.ED (Science) - Double Mathematics, in 2005 from Egerton University (Kenya), M.Sc. in Applied Mathematics in 2013 from Kenyatta University (Kenya), and Ph.D. in Applied Mathematics from Moi University (Kenya) in 2017.

C. G. Ngari also obtained Certified Public Accountant one (CPA 1) from KASNEB (Kenya).

C. G. Ngari has twelve years teaching experience at Secondary school level and five years experience at university level. Since January 2018, C. G. Ngari has been with the University of Embu (Kenya) as a Lecturer.

C. G. Ngari's research interest lies in Mathematical Modelling, Analysis and Simulations.